

*Università di Padova - Dipartimento di Ingegneria dell'Informazione,  
via Gradenigo 6/b 35131 Padova (Italy)*

*Tel. +39.049.827.7600*

*Fax +39.049.827.7699*

**TID and SEE Report on  
Micron MT29F16G08ABABA  
Single-Level-Cell NAND Flash Memory**

**Authors:** Marta Bagatin, Simone Gerardin, Alessandro Paccagnella, Università di Padova

The work described in this report was done under  
ESA Contract 4000103347/11/NL/PA  
"Studies of radiation effects in new generation of non-volatile memories"

Technical officer: Véronique Ferlet-Cavrois, ESA ESTEC, TEC-QEC

**v1.0**

**Date:** March 2013

# TABLE OF CONTENTS

1	Introduction.....	4
2	Applicable and Reference Documents.....	4
3	Tested Devices.....	4
4	Total Ionizing Dose (TID) Tests.....	5
4.1	Experimental Conditions.....	5
4.2	Experimental Results.....	7
4.2.1	Retention.....	7
4.2.2	Erase/Read/Program/Read Loops.....	7
4.2.3	Supply Current during Irradiation.....	9
4.2.4	Failure Doses: Summary.....	9
4.2.5	Post-radiation Annealing.....	10
5	Single Event Effects (SEE) Tests.....	11
5.1	Experimental Conditions.....	11
5.2	Experimental Results.....	13
5.2.1	Floating Gate Errors.....	13
5.2.2	SEFIs.....	14
5.3	Error-rate Calculations.....	16
6	Conclusions.....	18

## FIGURES

Figure 1: Irradiation setup.....	6
Figure 2: Byte errors in retention cells as a function of dose. ....	7
Figure 3: Number of block erase fails versus dose. ....	8
Figure 4: Block erase time versus dose. ....	8
Figure 5: Number of errors detected in the read after erase versus dose. ....	8
Figure 6: Page read time (after erase) versus dose. ....	8
Figure 7: Number of page program fails versus dose. ....	9
Figure 8: Page program time versus dose. ....	9
Figure 9: Number of errors detected in the read after program versus dose. ....	9
Figure 10: Page read time (after program) versus dose. ....	9
Figure 11: Supply current during program as a function of dose during irradiation. ....	10
Figure 12: Failure doses for erase, program, check after erase, check after program, and retention errors (1% of the irradiated cells). ....	10
Figure 13: Heavy-ion induced Floating Gate Errors Bit Cross Section as a function of LET (Sample MF28 for high-LET ions, Sample MF29 for high-energy ions). ....	14
Figure 14: Proton induced Floating Gate Errors Bit Cross Section as a function of energy. Errors bars are smaller than the symbols, except for MF34. ....	14
Figure 15: SEFI device cross section with heavy ions. (Errors bars are at 95% confidence interval. When no errors are recorded, empty symbols indicate minimum measurable cross section). ....	15
Figure 16: SEFI device cross section with protons. (Errors bars are at 95% confidence interval. When no errors are recorded, empty symbols indicate minimum measurable cross section). ....	15

## TABLES

Table 1: Details of the SLC NAND memories used for this work. ....	4
Table 2: Gamma TID runs performed at ESA/ESTEC Co-60 source and x-ray tests performed at the Laboratori Nazionali di Legnaro (LNL). ....	5
Table 3: Heavy-ion beams and test conditions used at HIF. ....	12
Table 4: Proton beams and test conditions used at PIF. ....	13
Table 5: Error rate calculations. ....	16
Table 6: Uncorrectable bit error rate as a function of raw bit error rate, using a 4-bit ECC per 540 bytes. ....	17
Table 7: Summary of the observed effects during TID tests. ....	18
Table 8: Summary of the observed effects during heavy-ion irradiations. ....	18
Table 9: Summary of the observed effects during proton irradiations. ....	18

## 1 Introduction

Under ESA Contract 4000103347/11/NL/PA “Studies of radiation effects in new generation of non-volatile memories”, we evaluated total dose and single event effects in Micron MT29F16G08ABABA Single-Level-Cell Flash Memories.

NAND Flash memories are based on Floating Gate (FG) cells and they are currently the leading technology in the market of large-size non-volatile memories. Single-Level Cell (SLC) Flash memory stores one memory bit in each FG cell.

## 2 Applicable and Reference Documents

- ESCC22900 Total Ionizing Dose (TID) Testing
- ESCC25100 Single Event Effects (SEE) Testing
- Micron MT29F16G08ABABA NAND Flash Memory datasheet

## 3 Tested Devices

For this work we used one-bit-per-cell 16-Gbit Flash memories manufactured by Micron with a 34-nm feature size. The details of the tested samples are reported in **Table 1**.

<b>Internal reference number</b>	MF2 MF3 MF5 MF7 MF8 MF9 MF10 MF37 MF39 MF40 MF41 MF42	MF28 MF29	MF34 MF45 MF47	MF1
<b>Part number</b>	MT29F16G08ABAB A	MT29F16G08ABAB A	MT29F16G08ABAB A	MT29F16G08ABAB A
<b>Supply voltage</b>	2.7V-3.6V	2.7V-3.6V	2.7V-3.6V	2.7V-3.6V
<b>Density</b>	16 Gbit	16 Gbit	16 Gbit	16 Gbit
<b>Minimum required ECC</b>	4-bit ECC per 540 bytes of data	4-bit ECC per 540 bytes of data	4-bit ECC per 540 bytes of data	4-bit ECC per 540 bytes of data
<b>Package</b>	48-pin TSOP	48-pin TSOP, decapped	48-pin TSOP	48-pin TSOP
<b>Operating temp</b>	0°C to +70°C	0°C to +70°C	0°C to +70°C	0°C to +70°C
<b>Lot code</b>	Unknown	Unknown	Unknown	Unknown
<b>Package markings</b>	I006 I-2 29F16G08ABABA- WP B	I006 I-2 29F16G08ABABA- WP B	I006 I-2 29F16G08ABABA- WP B	I006 I-2 29F16G08ABABA- WP B
<b>Die markings</b>	n.a.	n.a. (corners of the die are not exposed)	n.a.	n.a.
<b>Test</b>	TID	Heavy ions	Protons	Reference

**Table 1:** Details of the SLC NAND memories used for this work.

## 4 Total Ionizing Dose (TID) Tests

### 4.1 Experimental Conditions

Irradiations were performed using the Co60 source at ESA/ESTEC (Noordwijk, The Netherlands). Two TID test campaigns were performed, one in June 2011 and the other one in December 2011. A dose rate of about 1.4 rad/s(Si) was used.

In addition, a further test campaign was performed using a 10-keV x-ray probe station at the Laboratori Nazionali di Legnaro, LNL (Padova, Italy). A dose rate of 10 rad/s(Si) has been used.

The main experimental details concerning TID tests are summarized in **Table 2**.

The used test setup consists of an FPGA motherboard controlled by a host PC and a daughterboard with an open-top socket, where the Device Under Test (DUT) is placed. The connection between the two boards is implemented through a couple of high-speed connectors. The supply current drawn by the memory under test is constantly monitored through a PC-controlled multimeter and stored on log. A PC-controlled power supply is used to supply the DUT.

A schematic illustration of the irradiation setup is shown in **Fig. 1**. The FPGA controlling board is protected from gamma rays through proper shielding bricks available at the ESTEC Co60 facility.

During the TID tests, 1 Gbits for each memory were exercised with Erase/Read/Program/Read (E/R/P/R) loops, whereas another portion (again 1 Gbit) was kept in retention mode and periodically read.

Run	Start	Stop	Source	Dose rate(Si) [rad/s]	Dose(Si) [krad(Si)]	DUTs	Operating conditions
2_A	28/06/2011 10.42	29/06/2011 11.24	ESTEC Co <sup>60</sup>	1.3775	122.5	MF37	High duty cycle
4_A	29/06/2011 19.07	30/06/2011 11.52	ESTEC Co <sup>60</sup>	1.3785	83.2	MF39	Low duty cycle
6_A	30/06/2011 15.05	30/06/2011 15.23	ESTEC Co <sup>60</sup>	1.373	1.5	MF40	High duty cycle
7_A	30/06/2011 15.25	01/07/2011 9.14	ESTEC Co <sup>60</sup>	1.37575	88.2	MF40	High duty cycle
12_A	01/07/2011 16.24	01/07/2011 19.08	ESTEC Co <sup>60</sup>	1.3775	122.5	MF42	Low duty cycle
13_A	01/07/2011 19.14	04/07/2011 9.18	ESTEC Co <sup>60</sup>	1.3785	83.2	MF42	Low duty cycle
1_B	02/12/2011 16.37	03/12/2011 12.49	ESTEC Co <sup>60</sup>	1.4115	102.6	MF5 MF7	Unbiased Unbiased
2_B	03/12/2011 12.56	04/12/2011 12.16	ESTEC Co <sup>60</sup>	1.419	119.2	MF5 MF7	Unbiased Unbiased
3_B	04/12/2011 12.49	05/12/2011 15.34	ESTEC Co <sup>60</sup>	1.418	136.5	MF8	Unbiased
4_B	05/12/2011 15.59	06/12/2011 11.01	ESTEC Co <sup>60</sup>	1.4185	97.1	MF9 MF10	Low duty cycle High duty cycle
1_C	23/02/2012 10.17	23/02/2012 15.09	LNL x rays	10	174.7	MF2	High duty cycle
2_C	27/02/2012 17.46	27/02/2012 21.58	LNL x rays	10	134.9	MF3	High duty cycle

**Table 2:** Gamma TID runs performed at ESA/ESTEC Co-60 source and x-ray tests performed at the Laboratori Nazionali di Legnaro (LNL).

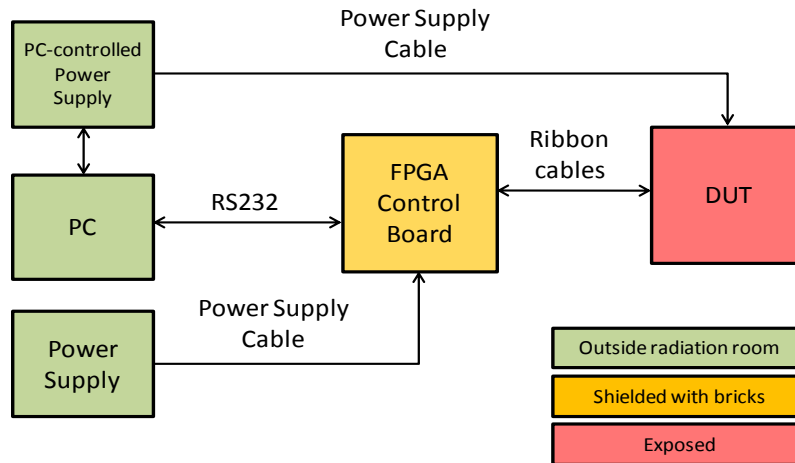


**Figure 1:** Irradiation setup.

Different operating conditions were used during the tests:

- **High-duty cycle**, with continuous Erase/Program operations to maximize the use of cells, charge pumps, and control circuitry. In particular the following sequence of operations was implemented:
  - 1 10 E/R/P/R loops with pseudo-random patterns (duration ~ 50 s)
  - 2 Read of the cells kept in retention (few s)
  - 3 Go to 1 if no failure
- **Low-duty cycle**, with the memory performing Erase/Program operation less than 0.2 % of the time. In particular the following sequence of operations was implemented:
  - 1 10 E/R/P/R loops with pseudo-random patterns (duration ~ 50 s)
  - 2 1 read of the cells kept in retention (few s)
  - 3 Memory in standby for 25 minutes
  - 4 Go to 1 if no failure
- **Unbiased**: same as for low-duty cycle, except for 3:
  - 3 Memory unbiased for 25 minutes

Concerning the cells kept in retention, no refresh operations were performed during all kinds of irradiations, high- and low-duty cycles and unbiased irradiations. After each erase, program, and read operation, different parameters/signals were monitored during irradiation:

- The Status Register (SR), which signals if program and erase operations have been successfully performed.
- The Ready/Busy (RB) signal, which is a device output that indicates if the memory is busy or ready to accept new commands. For instance, during a program operation the RB signal is active (low); as soon as the operation is completed, the RB goes inactive (high).

In detail:

- After erase operations we logged:
  - SR, to detect erase fails;
  - RB low time, to measure the erase time;
- After each program operation we logged:
  - SR, to detect program fails;
  - RB low time, to measure the program time;
- After each read operation we logged:
  - RB low time, to measure the read time;
  - Number and location of errors.

Finally, for cells kept in retention during dynamic tests, we logged the number and location of errors.

## 4.2 Experimental Results

### 4.2.1 Retention

**Fig. 2** shows the error build-up in FG cells kept in retention mode as a function of dose, for memories irradiated with high-duty cycle, low-duty cycle, and unbiased conditions. A sharp increase in the number of retention errors occurs after 65 krad(Si). As we will see later, there is practically no dependence on the irradiation conditions, even though **Fig. 2** seems to suggest that unbiased devices tend to show retention errors at higher doses.

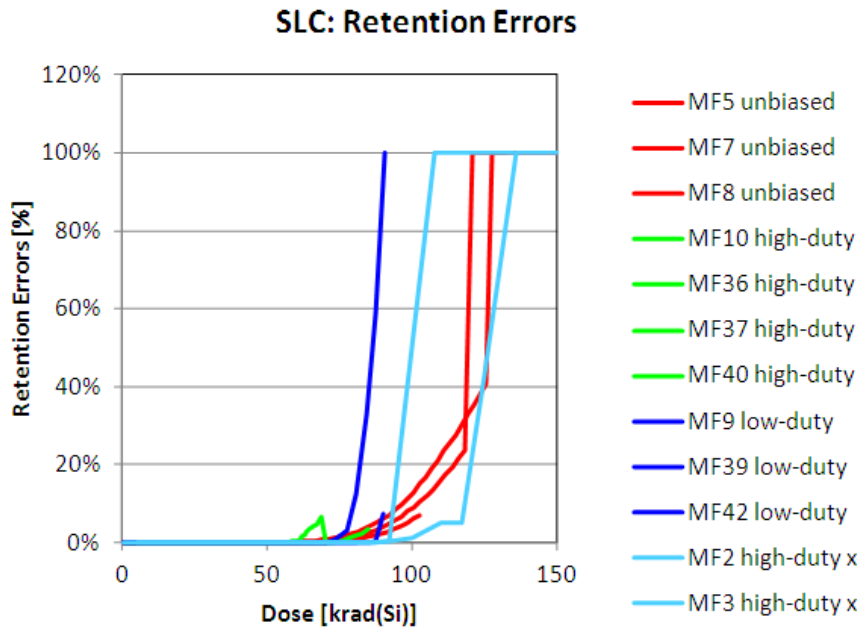


**Figure 2:** Byte errors in retention cells as a function of dose.

### 4.2.2 Erase/Read/Program/Read Loops

**Fig. 3** plots the number of erase fails as a function of dose, for memories irradiated in high-duty cycle, low-duty cycle, and unbiased conditions. This kind of errors is detected when the SR signals that an erase operation has not been successfully carried out. Erase errors appear between 60 and 75 krad(Si) in high- and low-duty cycle devices, whereas they begin after 115 krad(Si) in unbiased ones.

**Fig. 4** shows the block erase time as a function of dose, for memories irradiated in high-duty cycle, low-duty cycle, and unbiased conditions. The time to erase increases with increasing dose for high- until the erase operation fails (see Fig. 3). The variation of the block erase time in a reference non-irradiated sample subject to the same high-duty cycle loop as the irradiated samples is negligible.

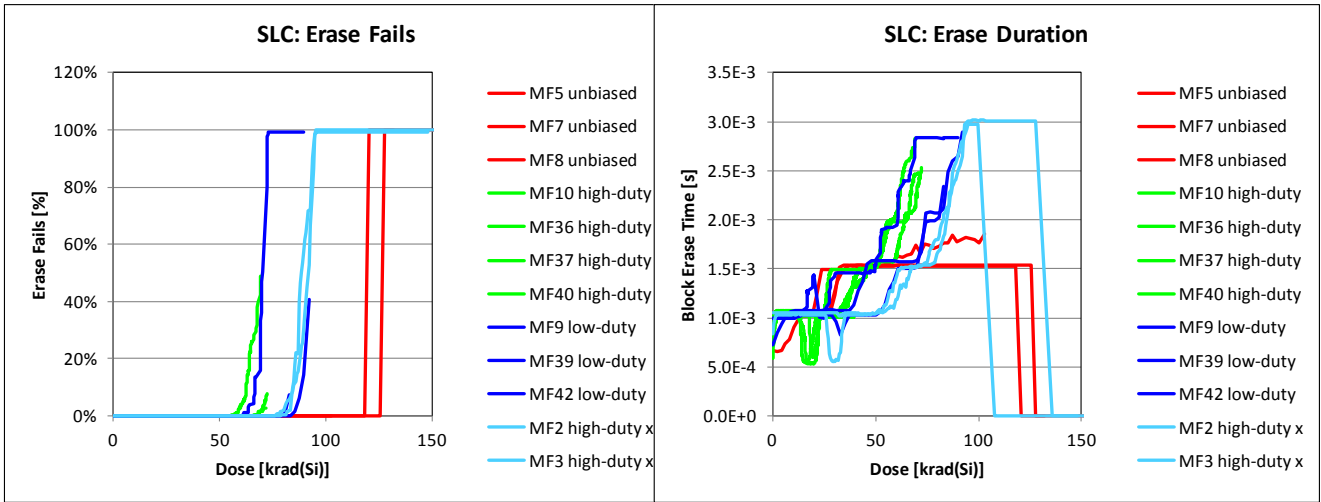


**Figure 3:** Number of block erase fails versus dose.

**Figure 4:** Block erase time versus dose.

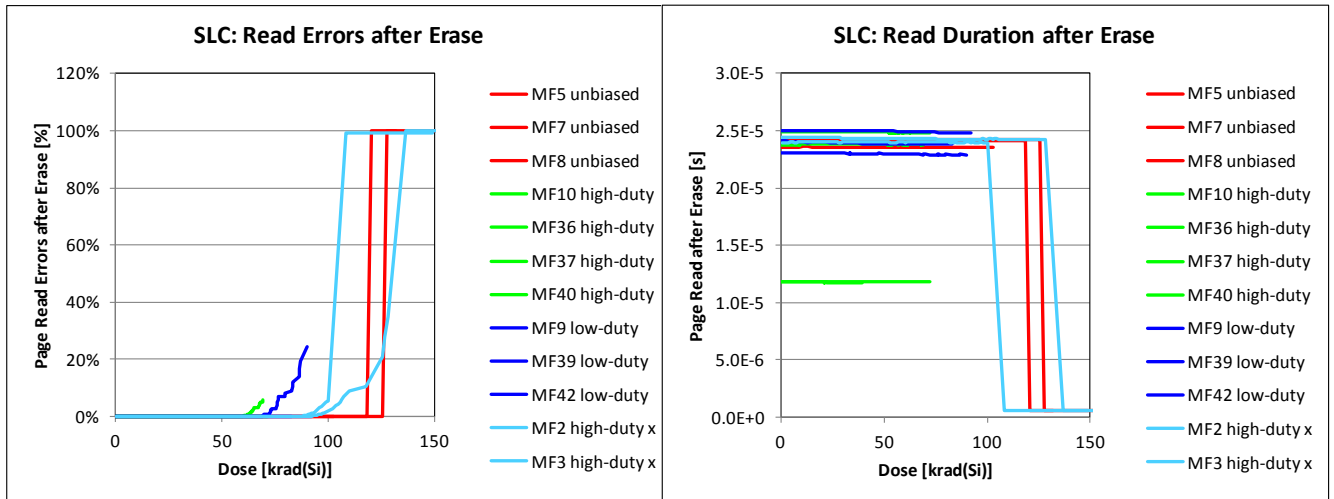


**Figure 5:** Number of errors detected in the read after erase versus dose.

**Figure 6:** Page read time (after erase) versus dose.

**Fig. 5** shows the number of errors detected in the read after erase, for memories irradiated in high-duty cycle, low-duty cycle, and unbiased conditions. Errors appear between 65 krad(Si) and 120 krad(Si), depending on duty cycle and radiation source.

**Fig. 6** shows the page read time (after erase) as a function of dose, for memories irradiated in high-duty cycle, low-duty cycle, and unbiased conditions. Practically no variations are detected in the read time before functional failures. The variation of the page read time in a reference non-irradiated sample subject to the same high-duty cycle loop as the irradiated samples is negligible.

**Fig. 7** depicts the number of program errors as a function of dose, for memories irradiated in high-duty cycle, low-duty cycle, and unbiased conditions. This kind of errors occurs when the SR signals that a program operation has not been successfully carried out. Program fails appear after 85 krad(Si).

**Fig. 8** illustrates the page program time as a function of dose, for memories irradiated in high-duty cycle, low-duty cycle, and unbiased conditions. The variation of the page program time in a reference non-irradiated sample subject to the same high-duty cycle loop as the irradiated samples is negligible.

**Fig. 9** shows the number of errors detected in the read after program, for memories irradiated in high-duty cycle, low-duty cycle, and unbiased conditions. Errors appear between 65 krad(Si) and 120-130 krad(Si), depending on duty cycle and radiation source.

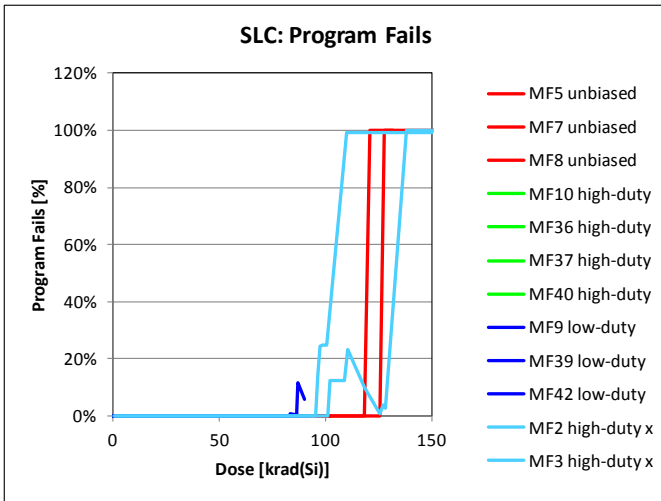


Figure 7: Number of page program fails versus dose.

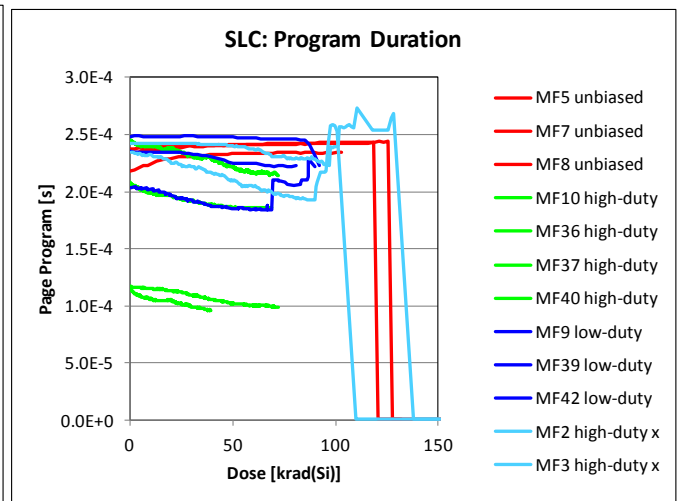


Figure 8: Page program time versus dose.

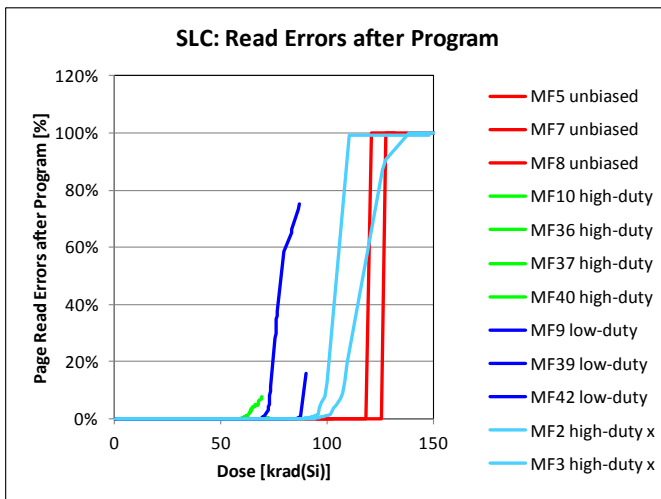


Figure 9: Number of errors detected in the read after program versus dose.

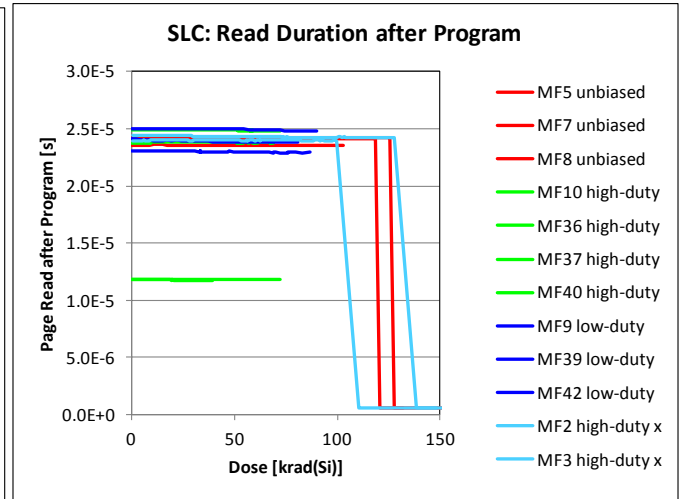


Figure 10: Page read time (after program) versus dose.

Fig. 10 shows the page read time (after program) as a function of dose, for memories irradiated in high-duty cycle, low-duty cycle, and unbiased conditions. The variation of the page read time in the reference non-irradiated sample subject to the same high-duty cycle loop as the irradiated samples is negligible.

#### 4.2.3 Supply Current during Irradiation

Fig. 11 shows the supply current during program as a function of dose. A moderate increase is visible, irrespective of the operating conditions.

#### 4.2.4 Failure Doses: Summary

Fig. 12 summarizes the average failure doses for erase errors, program errors, read errors after erase, read errors after program, and retention errors, for devices operated in the three conditions. For erase, program, and check errors, the higher the duty cycle the higher the failure dose. On the contrary, for retention errors, the failure dose only marginally depends on the duty cycle during irradiation.

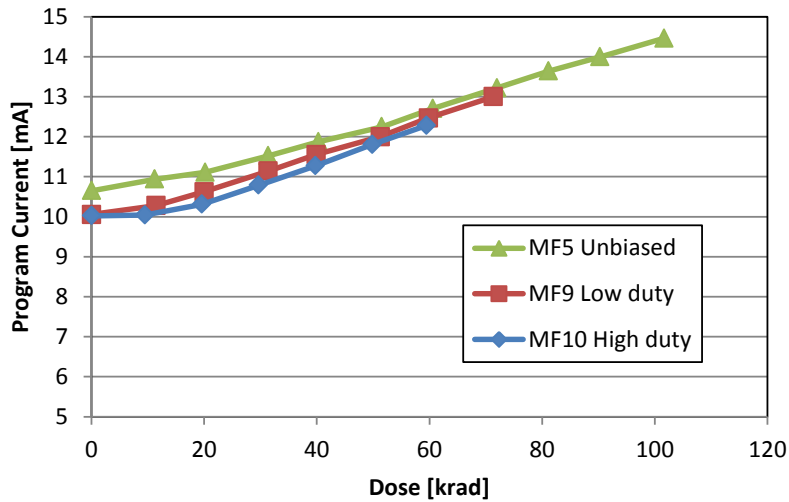


Figure 11: Supply current during program as a function of dose during irradiation.

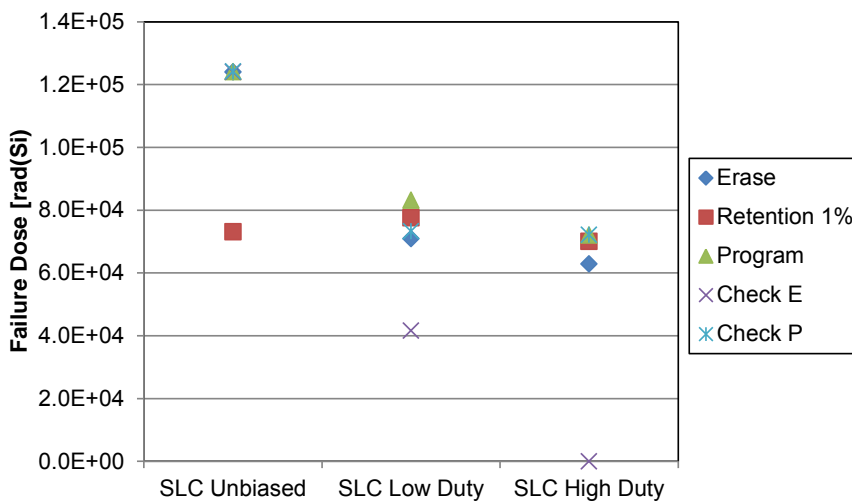


Figure 12: Failure doses for erase, program, check after erase, check after program, and retention errors (1% of the irradiated cells).

#### 4.2.5 Post-radiation Annealing

After the gamma exposure, samples MF36, MF37, MF39, MF40, and MF42 were stored for 1 week at room temperature with shorted pins. Then the memories were tested again: no recovery was observed. Afterwards, the same samples were baked at 100°C for 1 week at the University of Padova, with shorted pins. Again no recovery was observed.

All the samples were stored at room temperature after the exposure and/or annealing and were tested (read/erase/program) again about 21 months after irradiation (MF36, MF37, MF39, MF40, MF42) or about 15 months after irradiation (MF5, MF7, MF8, MF9, MF10). No functionality recovery was observed.

It is worth to note that the TID exposures were not stopped immediately after failure, but continued until access to the facility was possible (e.g. if a failure occurred during the night, the exposure was actually stopped the morning after). As a result, the doses after which the samples were stored at room temperature may be significantly larger than the failure doses indicated in Fig. 12.

## 5 Single Event Effects (SEE) Tests

### 5.1 Experimental Conditions

Heavy-ion irradiations were performed at the Heavy-Ion Facility (HIF) in Louvain-la-Neuve, Belgium, using the beams listed in **Table 3**. Proton irradiations were performed at the Proton Irradiation Facility (PIF) in Villigen, Switzerland, using the beams listed in **Table 4**.

The test setup for heavy ions consists of an FPGA motherboard controlled by a host PC and a daughterboard with an open-top socket, where the DUT is placed. The only difference with the TID setup described in Section 4.1 is that for heavy-ion tests there is no need of relatively long cables between the FPGA board and the daughterboard. The test setup for protons is virtually identical to the one used for total dose tests.

Both biased and unbiased conditions were used during heavy-ion and proton irradiations.

For the biased tests, the samples were exercised in different operating modes:

- Standby with active chip enable (only heavy ions)
- Erase/Read/Program/Read (E/R/P/R) loops

Ion Species	Cocktail	Energy [MeV]	EFF. LET [MeV cm <sup>2</sup> /mg]	Angle [°]	Memory condition	Monitored effects
N	High LET	60	3.30	0	Unbiased	FG errors
			3.42	15	Unbiased	FG errors
			3.81	30	Unbiased	FG errors
			5.13	50	Unbiased	FG errors
			3.30	0	E/R/P/R	SEFIs
Ne	High LET	78	6.40	0	Unbiased	FG errors
			7.39	30	Unbiased	FG errors
			9.05	45	Unbiased	FG errors
			9.96	50	Unbiased	FG errors
			6.40	0	E/R/P/R	SEFIs
Ar	High LET	151	15.90	0	Unbiased	FG errors
			18.36	30	Unbiased	FG errors
			22.49	45	Unbiased	FG errors
			24.74	50	Unbiased	FG errors
			15.90	0	E/R/P/R	SEFIs
Kr	High LET	305	15.90	0	Standby sel.	Destructive events
			40.40	0	Unbiased	FG errors
			41.83	15	Unbiased	FG errors
			46.65	30	Unbiased	FG errors
			57.13	45	Unbiased	FG errors
			40.40	0	E/R/P/R	SEFIs
			40.40	0	Standby sel.	Destructive events

Ion Species	Cocktail	Energy [MeV]	EFF. LET [MeV cm <sup>2</sup> /mg]	Angle [°]	Memory condition	Monitored effects
Ne	High energy	235	3	0	Unbiased	FG errors
			3.11	15	Unbiased	FG errors
			3.46	30	Unbiased	FG errors
			4.24	45	Unbiased	FG errors
			6	60	Unbiased	FG errors
Ar	High energy	372	10.2	0	Unbiased	FG errors
			10.56	15	Unbiased	FG errors
			11.78	30	Unbiased	FG errors
			14.42	45	Unbiased	FG errors
			20.4	60	Unbiased	FG errors
Ni	High energy	567	20.4	0	Unbiased	FG errors
			21.12	15	Unbiased	FG errors
			23.56	30	Unbiased	FG errors
			28.85	45	Unbiased	FG errors
			40.8	60	Unbiased	FG errors
Kr	High energy	756	32.6	0	Unbiased	FG errors
			33.75	15	Unbiased	FG errors
			37.64	30	Unbiased	FG errors
			46.1	45	Unbiased	FG errors
			65.2	60	Unbiased	FG errors

**Table 3:** Heavy-ion beams and test conditions used at HIF.

After each erase, program, and read operation during the E/R/P/R loops, different parameters were monitored under irradiation (see total dose section for further details). In particular:

- After erase operations we logged:
  - SR, to detect erase fails;
  - RB low time, to measure the erase time;
- After each program operation we logged:
  - SR, to detect program fails;
  - RB low time, to measure the program time;
- After each read operation we logged:
  - RB low time, to measure the read time;
  - Number and location of errors.

For the unbiased tests, the memories were exposed unbiased and programmed and read out of the beam.

Overall, 2 SLC NAND Flash memories were measured under heavy-ion irradiation, one with the high-LET cocktail and another one with the high-energy cocktail; 3 devices were measured under proton irradiation.

Ion Species	Energy [MeV]	Memory condition	Monitored effects
p	29.4	Unbiased	FG errors
p	47.2	Unbiased	FG errors
p	60.9	Unbiased	FG errors
p	101.4	Unbiased	FG errors
p	151.2	Unbiased	FG errors
p	200	Unbiased	FG errors
p	29.4	E/R/P/R	SEFIs
p	47.2	E/R/P/R	SEFIs
p	60.9	E/R/P/R	SEFIs
p	101.4	E/R/P/R	SEFIs
p	151.2	E/R/P/R	SEFIs
p	200	E/R/P/R	SEFIs

**Table 4:** Proton beams and test conditions used at PIF.

## 5.2 Experimental Results

Floating gate errors and SEFIs were observed both with heavy ions and protons, whereas the devices did not exhibit any latchup.

### 5.2.1 Floating Gate Errors

Floating Gate (FG) errors induced by heavy ions were measured with the device unbiased, with both normal and tilted irradiations. The FG error cross section per bit is illustrated in **Fig. 13**, as a function of the effective LET, for the two ion cocktails used at HIF, high LET and high energy. Error bars are smaller than the symbols in **Fig. 13**.

The heavy-ion cross section curve has been fitted with a Weibull function having the following parameters:

threshold LET:  $L_0=2.85 \text{ MeV}\cdot\text{mg}^{-1}\cdot\text{cm}^2$   
width:  $W =38 \text{ MeV}\cdot\text{mg}^{-1}\cdot\text{cm}^2$   
exponent:  $s=1.1$   
saturation:  $A=1.6\cdot 10^{-10} \text{ cm}^2$

Errors induced by protons have been measured with the device unbiased. The FG error cross section per bit after proton irradiation is illustrated in **Fig. 14**. Sample MF34 has a larger proton cross section than the other two. However, the number of errors collected on this sample is lower, and the statistical error (95% confidence) can explain the difference.

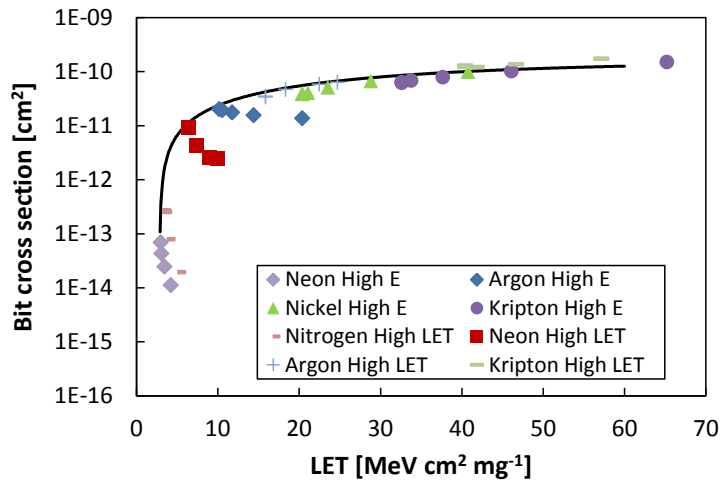


**Figure 13:** Heavy-ion induced Floating Gate Errors Bit Cross Section as a function of LET (Sample MF28 for high-LET ions, Sample MF29 for high-energy ions).

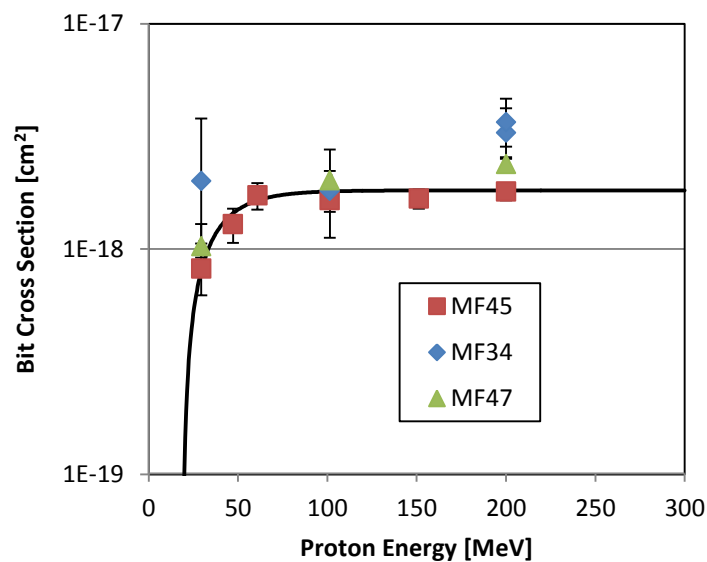


**Figure 14:** Proton induced Floating Gate Errors Bit Cross Section as a function of energy. Errors bars are smaller than the symbols, except for MF34.

The proton cross section curve for the sample with the best statistics (MF45) has been fitted with a Weibull function having the following parameters:

threshold energy:  $E_0=19$  MeV  
width:  $W=18$  MeV  
exponent:  $s=1$   
saturation:  $A=1.82 \cdot 10^{-18}$  cm<sup>2</sup>

### 5.2.2 SEFIs

Single Event Functional Interrupts (SEFI) were measured using heavy ions with the devices irradiated at normal incidence, during repeated Erase/Read/Program/Read (ERPR) loops. **Fig. 15** shows the device SEFI cross section versus ion LET. The empty symbol means that no errors have been observed (observability limit), up to a fluence of  $1 \cdot 10^7$  ions/cm<sup>2</sup>.

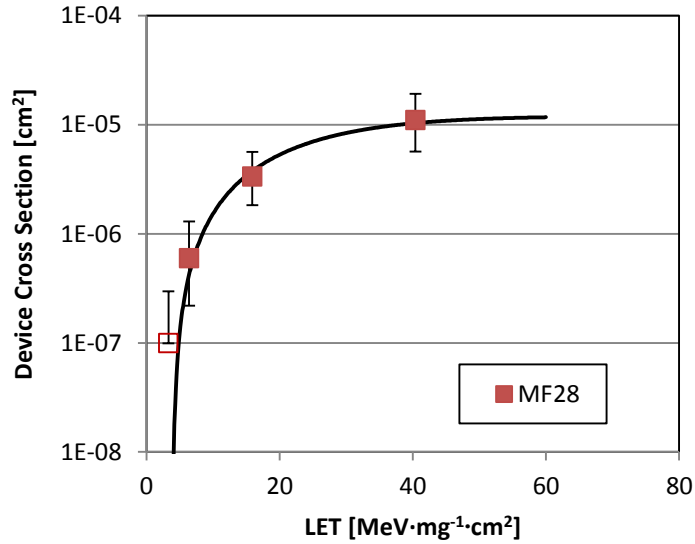


**Figure 15:** SEFI device cross section with heavy ions. (Errors bars are at 95% confidence interval. When no errors are recorded, empty symbols indicate minimum measurable cross section).

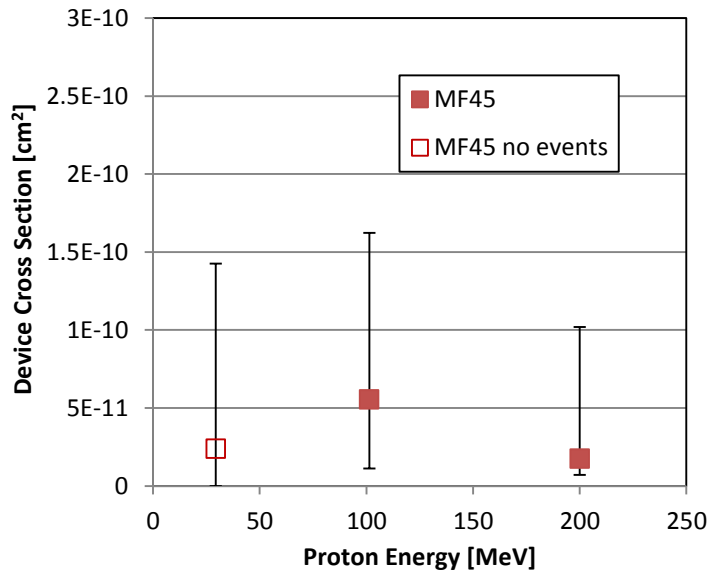


**Figure 16:** SEFI device cross section with protons. (Errors bars are at 95% confidence interval. When no errors are recorded, empty symbols indicate minimum measurable cross section).

The heavy ion cross section curve has been fitted with a Weibull function having the following parameters:

threshold LET:  $L_0=3.9 \text{ MeV}\cdot\text{mg}^{-1}\cdot\text{cm}^2$   
width:  $W =23 \text{ MeV}\cdot\text{mg}^{-1}\cdot\text{cm}^2$   
exponent:  $s=1.5$   
saturation:  $A=1.2\cdot 10^{-5} \text{ cm}^2$

SEFIs were also observed with protons. Due to the much smaller number of events, the determination of the cross section is less accurate than with heavy ions. **Fig. 16** shows the results as a function of proton energy.

### 5.3 Error-rate Calculations

Cremer96 has been used to calculate error rates in the following three orbits:

- 1) International Space Station (ISS) orbit
- 2) PROBA II orbit (LEO, perigee: 715.2 km, apogee: 735.1 km, inclination: 98.3 °)
- 3) Geosynchronous orbit.

Solar minimum, worst-day flare and peak 5 minutes flare have been used for the calculations. **Table 5** reports the results of error rate calculations. The depth of the sensitive volume is set to 100 nm for floating gate errors (i.e., the thickness of the floating gate). The floating gate error rates are calculated without ECC. A single node approximation with a 1- $\mu$ m thickness is used to calculate SEFI rates.

Orbit	ISS 51.6° 500 km	ISS 51.6° 500 km	ISS 51.6° 500 km	PROBA II 98.3° 715-735 km	PROBA II 98.3° 715-735 km	PROBA II 98.3° 715-735 km	GEO	GEO	GEO
Trapped protons	AP8min, avg flux			AP8min, avg flux					
Magnetic weather condition	quiet	quiet	quiet	quiet	quiet	quiet			
Solar conditions	solar min	flare, worst- day	flare, peak 5 minutes	solar min	flare, worst- day	flare, peak 5 minutes	solar min	flare, worst- day	flare, peak 5 minutes
Shielding	100 mils Al	100 mils Al	100 mils Al	100 mils Al	100 mils Al	100 mils Al	100 mils Al	100 mils Al	100 mils Al
Heavy-ion errors on programmed FG [ $\text{bit}^{-1} \cdot \text{s}^{-1}$ ]	5.97E-17	6.28E-14	2.27E-13	3.13E-16	2.78E-13	1.00E-12	1.32E-15	1.10E-12	3.95E-12
Proton errors on programmed FG [ $\text{bit}^{-1} \cdot \text{s}^{-1}$ ]	3.32E-17	2.74E-16	9.94E-16	9.74E-17	4.26E-15	1.55E-14	4.17E-19	2.22E-14	8.05E-14
Heavy-ion SEFIs [ $\text{s}^{-1}$ ]	2.80E-11	1.02E-08	3.72E-08	8.40E-11	7.00E-08	2.59E-07	2.93E-10	3.19E-07	1.19E-06
Proton SEFIs [ $\text{s}^{-1}$ ]	9.83E-10	7.39E-09	2.68E-08	2.94E-09	1.12E-07	4.06E-07	8.38E-11	5.80E-07	2.11E-06

**Table 5:** Error rate calculations.

Raw bit error rate	Uncorrectable bit error rate after ECC
1.00E-12	2.90E-48
1.00E-11	2.90E-43
1.00E-10	2.90E-38
1.00E-09	2.90E-33
1.00E-08	2.90E-28
1.00E-07	2.89E-23
1.00E-06	2.89E-18
1.00E-05	2.79E-13
1.00E-04	2.02E-08

**Table 6:** Uncorrectable bit error rate as a function of raw bit error rate, using a 4-bit ECC per 540 bytes.

The manufacturer specifies an ECC capable of correcting 4 bits per codeword of 540 bytes. **Table 6** can be used to estimate the uncorrectable error rate from the raw bit error rate, using the ECC specified by the manufacturer. In turn, the raw bit error rate is obtained by multiplying the rates in **Table 5** by the amount of time the memory has been exposed since the last write (ECC must cope with the number of errors accumulated since the last refresh or write).

## 6 Conclusions

**Table 7** summarizes the effects observed in the tested NAND SLC samples during TID irradiations with devices in different operating conditions and the dose at which those effects first appeared.

**Table 8** and **Table 9** show a summary for the events observed in the tested NAND SLC samples during heavy-ion and proton irradiation, respectively. As seen in **Table 8**, FG errors were observed starting from LET values of 3 MeV cm<sup>2</sup>/mg (the lowest used LET). The saturation cross section for FG errors is in the order of 10<sup>-10</sup> cm<sup>2</sup>. Floating gate errors due to protons have been observed at all tested energies (**Table 9**).

Observed effect	Memory operating condition	Av. failure gamma dose [krad(Si)]	Av. failure x-ray dose [krad(Si)]
Retention errors (in 1% of the tested cells)	High duty cycle loops, cells in retention without refresh	70	104
	Low duty cycle loops, cells in retention with refresh	78	-
	Unbiased, cells in retention without refresh	73	-
Failure of erase operation during E/R/P/R loops	High duty cycle E/R/P/R loops	63	78
	Low duty cycle E/R/P/R loops	71	-
	Unbiased	124	-
Errors after erase (in 10% of the tested cells)	High duty cycle E/R/P/R loops	n.a.	113
	Low duty cycle E/R/P/R loops	83	-
	Unbiased	124	-
Failure of program operation during E/R/P/R loops	High duty cycle E/R/P/R loops	72	98
	Low duty cycle E/R/P/R loops	83	-
	Unbiased	124	-
Errors after program (in 10% of the tested cells)	High duty cycle E/R/P/R loops	72	104
	Low duty cycle E/R/P/R loops	73	-
	Unbiased	124	-

**Table 7:** Summary of the observed effects during TID tests.

Observed effect	Operating condition	Threshold LET [MeV cm <sup>2</sup> /mg]	Saturation $\sigma$ [cm <sup>2</sup> ]
Floating Gate cell errors	Unbiased	< 3	~ 1.6E-10 per bit
SEFIs	E/R/P/R loops	>3, <6.4	~ 1E-5 per device

**Table 8:** Summary of the observed effects during heavy-ion irradiations.

Observed effect	Operating condition	Threshold Energy [MeV]	Max $\sigma$ [cm <sup>2</sup> ]
Floating Gate cell errors	Unbiased	< 29.4	~ 2e-18 per bit
SEFIs	E/R/P/R loops	< 101.4	~ 1e-10 per device

**Table 9:** Summary of the observed effects during proton irradiations.